Chemical Research in Toxicology

Article

pubs.acs.org/crt

Anionic Phenolic Compounds Bind Stronger with Transthyretin than Their Neutral Forms: Nonnegligible Mechanisms in Virtual Screening of Endocrine Disrupting Chemicals

Xianhai Yang, Hongbin Xie, Jingwen Chen,* and Xuehua Li

Key Laboratory of Industrial Ecology and Environmental Engineering (MOE), School of Environmental Science and Technology, Dalian University of Technology, Dalian 116024, China

Supporting Information

ABSTRACT: The molecular structures of many endocrine-disrupting chemicals (EDCs) contain groups that ionize under physiological pH conditions. It is unclear whether the neutral and ionic forms have different binding mechanisms with the macromolecular targets. We selected phenolic compounds and human transthyretin (hTTR) as a model system and employed molecular docking with quantum mechanics/molecular mechanics optimizations to probe the mechanisms. The binding patterns of ionizable ligands in hTTR crystal structures were also analyzed. We found that the anionic forms of the phenolic compounds bind stronger than the corresponding neutral forms with hTTR. Electrostatic and van de Waals interactions are the dominant forces for most of the anionic and neutral forms, respectively. Because of the dominant and orientational electrostatic interactions, the $-O^-$ groups point toward the entry port of the binding site. The aromatic rings of the compounds also form cation$-\pi$ interactions with the $-NH_3^+$ group of Lys 15 residues in hTTR. Molecular descriptors were selected to characterize the interactions and construct a quantitative structure−activity relationship model on the relative competing potency of chemicals with T_4 binding to hTTR. It is concluded that the effects of ionization should not be neglected when constructing *in silico* models for screening of potential EDCs.

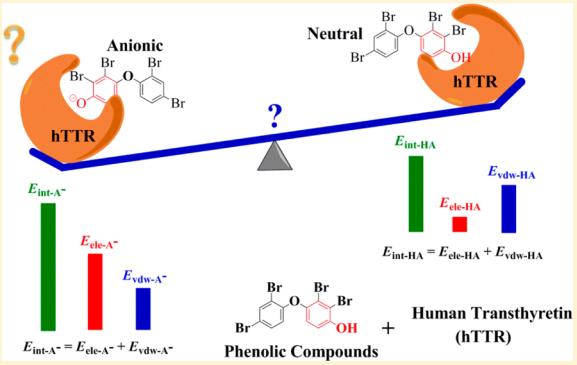

INTRODUCTION

Thyroid hormones (THs) regulate growth, differentiation, metamorphosis, and thermogenesis of vertebrates.[1] Under normal physiological conditions, THs need to be carried to their sites of action through transport proteins including transthyretin (TTR), thyroxine-binding globulin (TBG), and albumin to exert their biological effects in humans.[1,2] However, some organic chemicals termed thyroid-disrupting chemicals (TDCs) can disrupt the TH's transport process by competing for transport proteins with THs.[2,3] The TDCs bound to the TH carriers may be transported to normally inaccessible sites of action, e.g., the uterus and brain and therefore may decrease the TH level in the sites (Figure 1).[4,5] Thus, it is important to screen the potential TDCs from commercially used chemicals so as to decrease the possible impacts of those chemicals on the thyroid system. Understanding the disturbing mechanism of TDCs is a significant step toward this aim.

To date, hundreds of chemicals have been tested on the disrupting activities with the three TH carriers of humans.[4,6] The experimental results indicate that various TDCs have distinct binding potency with the three carriers. As the binding potency of 3,3′,5,5′-tetraiodo-L-thyronine (T_4) with human TBG (hTBG) was higher than that with human TTR (hTTR),[6] it is slightly easier for TDCs to compete for T_4 binding to hTTR than hTBG.[4,7] Moreover, hTTR is the major TH carrier in the brain and fetal tissues.[1,2,4] Therefore, disrupting the hTTR transport process is an important pathway for TDCs to alter THs homeostasis.

For almost all of the high potency hTTR disruptors, their molecular structures contain ionizable functional groups, e.g., −OH, −COOH, and $-SO_3H$. Especially, previous studies indicate that the phenolic −OH group is a key factor for strong binding to hTTR.[8] It is known that compounds with the ionizable groups can ionize depending on the pH of the environment and their pK_a. For ionizable compounds, their toxicity and mechanisms of action differ greatly with respect to the ionic or neutral forms.[9−11] Rendal et al. reviewed the acute toxicity and bioaccumulation of ionizable organic acids and bases, and concluded that the neutral forms of ionizable compounds are more toxic and more bioaccumulative than their corresponding ionic forms.[12] Similarly, for disrupting the hTTR transport process, we raised the following questions: do neutral and anionic forms of ionizable TDCs have different binding potency with hTTR? Is there any correlation between the pK_a of TDCs and their competitive interaction with T_4 binding to hTTR if the neutral and anionic forms of TDCs bind differently with hTTR?

Received: April 24, 2013
Published: August 13, 2013

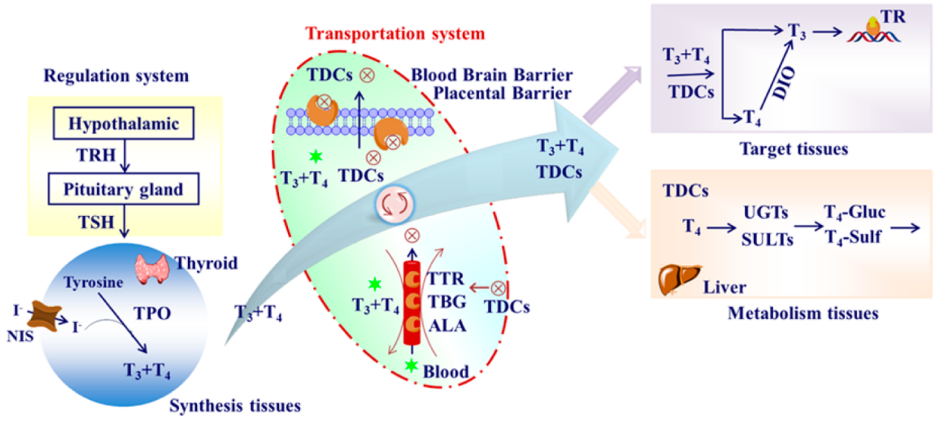

Figure 1. Role of the thyroid hormone transports in the thyroid hormone system. Abbreviations: DIO, deiodinases; NIS, sodium/iodide symporter; T_3, 3,3′,5-triiodo-L-thyronine; T_4, 3,3′,5,5′-tetraiodo-L-thyronine; TDCs, thyroid disrupting chemicals; TPO, thyroperoxidase; TR, thyroid receptor; TRH, thyrotropin-releasing hormone; TSH, thyroid-stimulating hormone; UGTs, glucuronosyltransferase; SULTs, sulfotransferase.

T_4 has three ionizable moieties (−COOH, −OH and $-NH_2$), and the corresponding pK_a values are 2.40, 6.87, and 9.96, respectively.[13] The −COOH group of T_4 ionizes in normal physiological pH conditions and forms ionic interactions with the $-NH_3^+$ group of the Lys 15 residue in hTTR.[14,15] Such ionic interactions play a determining role in T_4 binding with hTTR.[14,15] The −OH groups of many TDCs can ionize in normal physiological pH conditions. Therefore, the dissociated TDCs may also form ionic interactions with hTTR as exhibited by T_4. This may lead to different binding mechanisms for the neutral and anionic forms of TDCs with hTTR. However, there is no previous report on the binding mechanisms for dissociated TDCs with hTTR. Clarifying this binding mechanism is of vital importance to mechanistic *in silico* screening of potential hTTR disruptors.

In silico screening is increasingly viewed as a crucial part of the new toxicology test strategy for the 21st century.[16,17] For example, the European REACH (Registration, Evaluation, and Authorization, and Restriction of Chemicals) legislation that came into force in 2007 advocated the use of nonanimal testing methods such as *in silico* for chemical safety and ecological risk assessment.[18] In the United States, *in silico* tools for assessing chemical exposure, hazard, and risks are also being developed by the National Center for Computational Toxicology.[17]

To date, many *in silico* tools for chemicals regulatory purposes have been developed based on the methodology of quantitative structure−activity relationships (QSARs).[19] As the binding potency of TDCs with TTR is a potential regulatory end point,[5] it is necessary to construct mechanism-based predictive models to set priority and screen potential hTTR disruptors for regulatory purposes. Papa et al.,[20] Kovarich et al.,[8] and Yang et al.[21] developed QSAR models to characterize the binding potency of brominated flame-retardants with hTTR. Their results clarified that hydroxylated brominated flame-retardants can form hydrogen bonds with hTTR. Nevertheless, it is still unclear whether neutral or anionic forms of ionizable chemicals have different competitive interactions with T_4 binding to hTTR.

In the present study, phenolic chemicals were selected to unravel the binding mechanisms of different chemical forms with hTTR, as >75% of the chemicals that have been tested to exhibit stronger binding potency with hTTR than that of T_4 are phenolic compounds. We first investigated the possible correlation between the pK_a of phenolic compounds and the competitive potency of those chemicals with T_4 binding to hTTR. Then different interactions between the anionic/neutral forms of the phenolic compounds and hTTR were identified by analyzing their complex structures optimized by hybrid quantum mechanics/molecular mechanics (QM/MM) and the experimental hTTR crystal structures with ionizable ligands. At last, appropriate molecular descriptors were selected to characterize the interactions and to construct a mechanism-based QSAR model.

MATERIALS AND METHODS

Data Sets and Studied Compounds. Three sets of experimental data on the competing potency of chemicals were selected for the study (Table S1 of the Supporting Information). The competitive interaction of a chemical with T_4 binding to hTTR was determined by *in vitro* competitive binding assays, including the radiolabeled ligand displacement method, the competitive fluorescence displacement assay, and the surface plasmon resonance biosensor-based method.[6] Data set I includes 47 compounds (36 phenolic and 11 nonionizable compounds), for which the competing potency was tested by the radiolabeled ligand displacement method under the condition of pH 8.0.[7,22−27] Data set II includes 8 chlorinated phenols, for which the competing potency was determined by the same competitive binding assay as that for data set I but with pH 7.3.[28] Data set III includes 14 hydroxylated polybrominated diphenyl ethers (HO-PBDEs), for which the competing potency was determined by the competitive fluorescence displacement assay under the condition of pH 7.4 and 8-anilino-1-naphthalenesulfonic acid ammonium salt as fluorescence probes.[29] In total, there are 53 ionizable compounds in data sets I, II, and III. The end point for the three data sets is the half-maximal inhibitory concentration (IC_{50}), which represents the concentration of a chemical when it replaces 50% of T_4 bound to hTTR. Data set I was divided into a training set (38 compounds) and a validation set (validation set I, 9 compounds) through the splitting protocol described by Liu et al.[30] The training set was employed to develop QSAR models, and the validation set was used to evaluate the predictive ability of the model. Data sets II and III were also used as external validation sets (validation sets II and III) to further test the predictive ability of the developed QSAR model.

Molecular Modeling. Molecular modeling was employed to analyze the binding patterns of neutral and anionic forms of the phenolic compounds in the hTTR active site. Three successive steps of calculation were performed, including molecular docking, QM/MM optimization, and binding pattern analysis. All of the calculations except for the hydrophobic interaction analysis were performed with Discovery Studio 2.5.5 (Accelrys Software Inc.). The hydrophobic interaction was characterized by the LIGPLOT program.[31]

We only focused on the binding mechanism of the chemicals with hTTR in the activity site, and the kinetic process such as the permeation rate[32] was out of the scope of this study. The CDOCKER protocol was adopted in the molecular docking to determine the potential bioactive conformation for chemical binding to hTTR. The initial structure of hTTR for the molecular docking simulation was obtained by stripping the ligand T_4 from the hTTR crystal structure with the PDB ID 1ICT (tetramer, ligand T_4) that was selected from the Protein Data Bank.[33] As the experimental IC_{50} data were determined at different pH conditions, it is necessary to consider the different protonation states of the ionizable residues of hTTR in molecular docking. Here, the Prepare Protein protocol was employed to protonate or deprotonate the ionizable residues under the pH conditions of 8.0, 7.3 and 7.4 in data sets I, II, and III, respectively.

The conformation determined by the molecular docking was further optimized by the QM/MM minimization protocol. The QM/MM hybrid method can perform quantum mechanics calculations and obtain reliable charge descriptions on the site of interest (QM region). Here, the QM subsystem consisted of a phenolic compound, described at the BLYP/DNP level within DMol^3, while hTTR was treated with the CHARMm molecular mechanics force field. The same division for the QM and MM regions was also used in the previous studies for systems such as nicotinic receptor[34] and acid-sensing ion channels.[35] On the basis of the conformations from the QM/MM simulation, the nonbonded interaction energy (E_{int}) between the QM and MM regions was calculated. E_{int} is the sum of electrostatic (E_{ele}) and van der Waals interaction energies (E_{vdw}):

$$E_{int} = E_{ele} + E_{vdw} \quad (1)$$

Moreover, the binding patterns of the ligands in the simulated and crystal structures were analyzed. To test the reliability of the computational scheme, the root-mean-square deviation (RMSD)[36] for non-hydrogen atoms between the X-ray pose of T_4 in 1ICT and the simulated pose of T_4 in 1ICT was calculated. The calculated RMSD (1.56 Å) is lower than the acceptable criteria of <2.00 Å,[36,37] indicating the reliability of the employed molecular modeling method.

QSAR Modeling. The logarithm of the relative competing potency of a chemical with T_4 binding to hTTR (log *RP*) was employed for QSAR modeling, so as to decrease the possible biases of the IC_{50} values from different laboratories. *RP* is defined as

$$RP = \frac{IC_{50,T_4}}{IC_{50,competitor}} \quad (2)$$

On the basis of the results from the binding pattern analysis, 16 molecular descriptors (Table S2, Supporting Information) were selected to describe the interactions of the phenolic compounds with hTTR. The details for justifying the descriptor selection were presented in Table S2 (Supporting Information). Among the 16 descriptors, the logarithm of the *n*-octanol/water distribution coefficient (log *D*), molecular weight (M_w), and the number of halogen atoms (n_X) may characterize hydrophobic interactions. log *D* was calculated from the logarithm of the octanol−water partition coefficient (log K_{OW}) and pK_a by the following expression:[38]

$$\log D = \log K_{OW} - \log(1 + 10^{pH-pK_a}) \quad (3)$$

Five quantum chemical descriptors including the highest occupied molecular orbital energy (E_{HOMO}) and the lowest unoccupied molecular orbital energy (E_{LUMO}), the most positive net atomic charge on a hydrogen atom (qH^+), and the most negative net atomic charge on a carbon atom (qC^-) and on an oxygen atom (qO^-), were selected to characterize hydrogen bonding, electron donor−acceptor interactions, and electrostatic interactions. To consider the contribution of both the anionic and the neutral forms, adjusted values for five descriptors (E_{int}, E_{HOMO}, E_{LUMO}, qC^-, and qO^-) were calculated by the following equation:[10]

$$X_{adj} = \delta_{HA} \cdot X_{HA} + \delta_{A^-} \cdot X_{A^-} \quad (4)$$

$$\delta_{HA} = \frac{[HA]}{[HA] + [A^-]} = \frac{1}{1 + 10^{pH-pK_a}}$$
$$\delta_{A^-} = \frac{[A^-]}{[HA] + [A^-]} = \frac{10^{pH-pK_a}}{1 + 10^{pH-pK_a}} \quad (5)$$

where X_{HA} and X_{A^-} are the descriptors for the neutral and ionized forms, respectively, δ_{HA} and δ_{A^-} are the fractions of the neutral and ionized species at a given pH condition, respectively.

Experimental pK_a values are only available for 13 compounds (Table S1, Supporting Information). For the other compounds, pK_a values were calculated by SPARC, v4.6,[39] which was proved to be suitable for predicting pK_a.[40−42] We also compared the pK_a values predicted by SPARC, Discovery Studio 2.5.5, and those from SciFinder (https://scifinder.cas.org). The reliability of the three pK_a calculation methods was evaluated by calculating the mean absolute error (MAE) based on the 13 compounds with experimental pK_a values. The calculated MAE values for SPARC, Discovery Studio 2.5.5, and SciFinder are 0.368, 0.408, and 0.388, respectively. Therefore, all three methods are reliable, and the SPARC method is slightly better than the other two. For all of the phenolic compounds, their pK_a values from the different estimation methods are generally comparable except for seven hydroxylated polychlorobiphenyls that were underestimated by Discover Studio (Table S1, Supporting Information). Here, the experimental and SPARC pK_a values were employed for model development. log K_{OW} was calculated by EPI Suit 4.1.[43] I_A was calculated by DRAGON 6.0.[44] All of the quantum chemical descriptors were calculated by the Gaussian 09 program package.[45] The geometry optimizations of the studied ligands were performed at the B3LYP/6-311++G(d,p) level followed by the frequency analysis. The polarized continuum model (PCM) was used to account for the solvent effect of water.[46] Values for some molecular descriptors are listed in Table S7 (Supporting Information).

Partial least squares (PLS) regression was employed to construct QSAR models. The Simca-S (version 6.0, Umetri AB & Erisoft AB) software was employed for the PLS analysis. To remove redundant predictor variables, the variable selection procedure[47] described previously was followed. The statistical parameters R^2 (determination coefficient), cross-validated Q^2_{CUM} (the total variation of the dependent variables that can be predicted by all of the extracted PLS components), and external explained variance Q^2_{EXT},[48] were employed to assess goodness-of-fit, robustness, and predictive ability of the QSAR model. The applicability domain (AD) of the QSAR model was assessed by the Euclidean distance-based method that was incorporated into AMBIT Discovery (version 0.04) (http://ambit.sourceforge.net/download_ambitdiscovery.html).

RESULTS AND DISCUSSION

Correlations between pK_a and log *RP*. For an ionizable chemical, the concentration ratio of neutral [HA] to ionized form [A^-] is determined by its pK_a and pH, i.e.,

$$\frac{[A^-]}{[HA]} = 10^{pH-pK_a} \quad (6)$$

The pK_a values for the compounds in data sets I, II, and III range from 4.40 to 15.07. Thus, the compounds may ionize to different extent under the experimental pH conditions (pH 8.0, 7.3, and 7.4 for data sets I, II, and III, respectively). At a given pH condition, if A^- binds stronger with hTTR than HA, it would be expected that log *RP* (or −log $IC_{50,competitor}$) would increase with the decrease of pK_a for different compounds; otherwise, it would be expected that log *RP* increases with the increase of pK_a. As shown in Figure 2 and Figure S1 (Supporting Information), we do find there are statistically significant ($p < 0.005$) negative correlations between the experimental log *RP* values and pK_a of the phenolic compounds from data sets I, II, and III. The results imply that the anionic

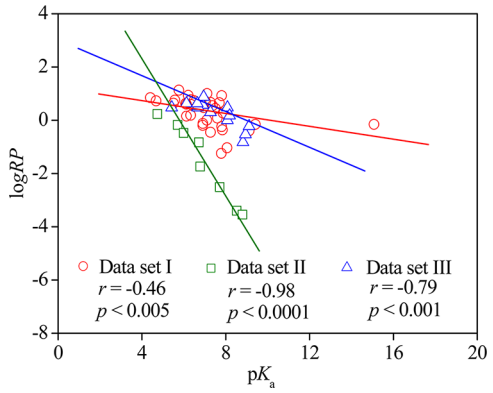

Figure 2. Correlation between log*RP* and pK_a for the three data sets of compounds under study.

forms of the phenolic compounds bind stronger with hTTR than the neutral forms.

Different Binding Mechanisms. The calculated E_{int} values for the neutral and anionic forms of the phenolic compounds are listed in Table S3 (Supporting Information). We found that the E_{int} values for the anionic forms are much lower than those of the corresponding neutral forms, which further confirms that the anionic forms bind stronger with hTTR than the neutral forms. Therefore, the binding affinity should be pH dependent based on eq 6. Pullakhandam et al. observed the phenomenon experimentally.[49]

Theoretically, log *RP* should have a good correlation with E_{int}. However, if only the neutral forms of the compounds are considered, no correlations between log *RP* and E_{int} ($p > 0.05$) can be observed. By considering the contributions of both the anionic and the neutral forms at a given pH condition, we calculate the adjusted interaction energy (E_{adj}) by eq 4. As can be seen from Figure 3 and Figure S2 (Supporting Information), the correlations between log *RP* and E_{adj} become statistically significant for the three data sets ($p < 0.05$). The results imply that the ionization should be considered in the computation of the interaction energy and development of *in silico* models for the screening of potential TTR disruptors.

The following binding pattern analysis unveils the mechanisms in which the anionic forms bind stronger with hTTR than the corresponding neutral forms. We first analyzed the most stable conformations in energy for the anionic and neutral forms in the T_4 binding channel of hTTR. For the anionic forms, we found that the ionized groups point toward the mouth of the T_4 binding site (Figure 4) for 43 compounds among the 53 phenolic compounds considered. In addition, we also analyzed 73 hTTR crystal structures with ionizable ligands (−OH, −COOH, $-SO_3H$ as end groups), which were collected from the Protein Data Bank.[33] Among these 73 crystal structures, there are 64 structures for which the ionizable ligands are estimated to be in the anionic forms under the experimental conditions. Among the 64 crystal structures, there are 58 structures for which the ionized groups ($-O^-$, $-COO^-$, $-SO_3^-$) point toward the mouth of the T_4 binding channel in hTTR (Table S4, Supporting Information). Thus, the simulation and crystal structural results indicate that in the dominant conformations of the anionic forms binding with hTTR, the ionized groups point toward the entry port of hTTR.

For the neutral forms, however, we can observe no dominant orientations for their ionizable groups. For example, our

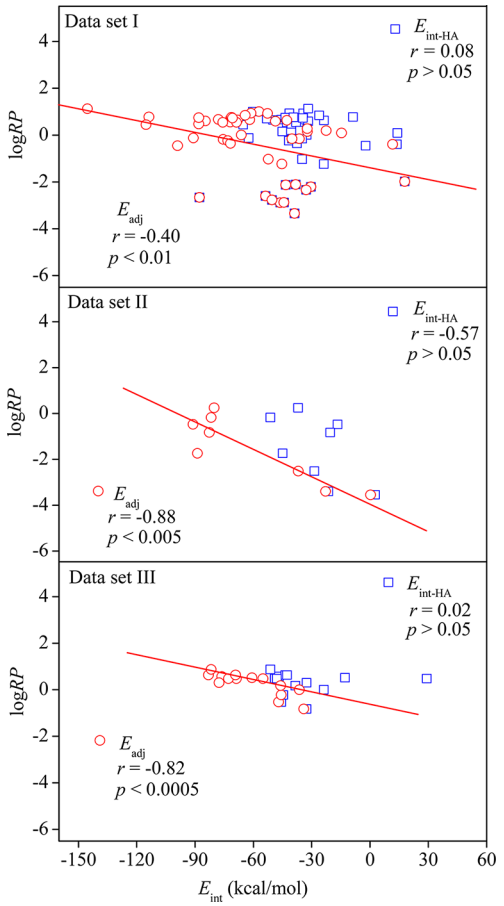

Figure 3. Relationship between log *RP* and interaction energy for the three sets of compounds under study.

simulation results show that among the 53 phenolic compounds, there are 34 compounds (in contrast to 43 when the chemicals are ionized) for which the −OH groups point toward the mouth of the T_4 binding channel in hTTR. In the hTTR crystal structures, 3 out of 9 neutral ligands point their ionizable groups toward the entry port.

Why do the ionized groups tend to orientate toward the entry port of hTTR? The $-NH_2$ group (pK_a = 10.5) at the side chain of the Lys 15 residue of hTTR can be protonated to form a $-NH_3^+$ group under normal physiological and experimental pH conditions (pH 7−8), and the $-NH_3^+$ group can form dominant and orientational electrostatic interactions with the anionic groups of the ligands.

According to Kumar and Nussinov,[50−53] if there exist stable electrostatic interactions in proteins, the distance between the anionic and cation groups is ≤5 Å. We analyzed the oxygen−nitrogen distances (d_{O-N}) between the ionized groups in the ligands and the $-NH_3^+$ group of Lys 15 based on the most stable conformations from the simulations and the hTTR crystal structures (Figure 5). Among the 53 compounds with −OH as end groups, we found that d_{O-N} of 45 compounds is ≤5 Å for the anionic forms. For the 64 crystal complexes with ionized ligands, d_{O-N} for 49 structures is ≤5 Å. These results further confirm that the anionic groups of the ligands form electrostatic interactions with the $-NH_3^+$ group of Lys15 in hTTR.

By analyzing the noncovalent interactions of the most stable conformations from the simulation and the hTTR crystal

dx.doi.org/10.1021/tx4001557 | *Chem. Res. Toxicol.* 2013, 26, 1340−1347

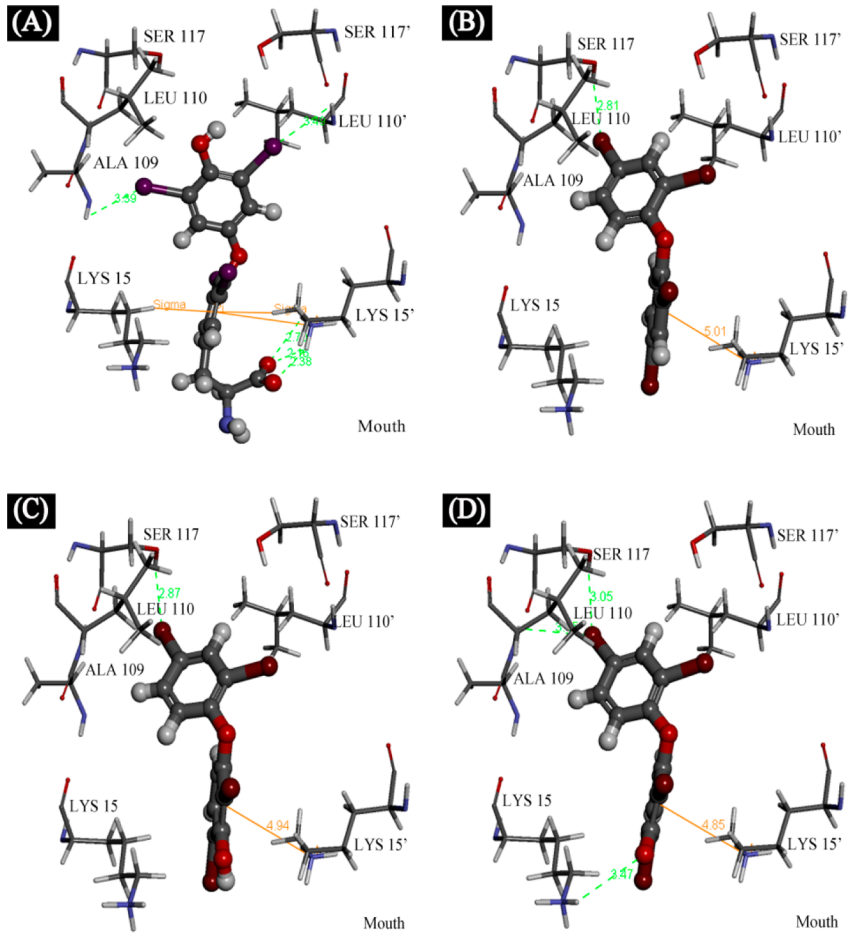

Figure 4. Conformations of T_4 (A), 2,2′,4,4′-tetrabrominated diphenyl ether (B), the neutral form of 3-*HO*-2,2′,4,4′-tetrabrominated diphenyl ether (C), and the anionic form of 3-*HO*-2,2′,4,4′-tetrabrominated diphenyl ether (D) adopted in the binding site of hTTR (1ICT). The green line and the orange line represent hydrogen bonds and cation−π interactions, respectively.

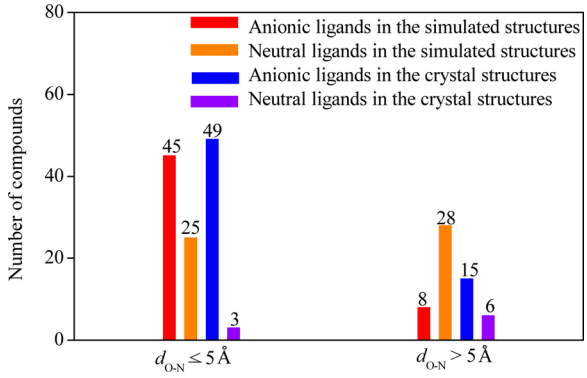

Figure 5. Distribution of the oxygen−nitrogen distances (d_{O-N}) between the ionizable groups in the ligands and the -NH_3^+ group of Lys 15.

structures, we also found that the $-NH_3^+$ group of Lys 15 residue can form cation−π interactions with the aromatic rings in the aromatic compounds (Figure 4 and Table S4, Supporting Information). The cation−π interactions were also observed in the dopamine transporter, glycine, and GABA 5-HT transporters, H^+-peptide transporter, and the human apical Na^+-dependent bile acid transporter.[54,55] The strength of the cation−π interactions can be qualitatively characterized by the electrostatic potential surfaces of the relevant aromatics, i.e., the more negative is the electrostatic potential surface on an aromatic ring, the stronger is the cation−π interaction.[56,57] For the phenolic compounds under study, the surface distribution of electrostatic potential for the anionic forms is more negative than that of the corresponding neutral forms (Figure S3, Supporting Information). Thus, the anionic forms of the phenolic compounds also have enhanced cation−π interactions with hTTR.

To further understand the nature of the difference in E_{int} between the anionic and neutral forms of the studied compounds, we compared the components of E_{ele} and E_{vdw} in E_{int} (Table S3 and Figure S4, Supporting Information). The results show that E_{ele} is lower than E_{vdw} for most of the anionic forms (9 exceptions), and E_{ele} is higher than E_{vdw} for most of the neutral forms (2 exceptions). Thus, electrostatic interactions are the dominant forces for most of the anionic forms binding with hTTR, whereas van de Waals interactions are dominant for most of the neutral forms. In addition, the ratios of E_{vdw} between the neutral and anionic forms are close to 1, implying that the van der Waals interactions for the anionic forms are similar to or slightly weaker than those of the corresponding neutral forms. However, for most of the compounds, the ratios of E_{ele} between the neutral and anionic forms are <0.5, suggesting that the electrostatic interactions for the anionic forms are much stronger than those of the corresponding neutral forms (3 exceptions). Therefore, the decreases in E_{ele} from the neutral to the anionic forms cause the

dx.doi.org/10.1021/tx4001557 | *Chem. Res. Toxicol.* 2013, 26, 1340−1347

anionic forms to have lower interaction energies (and stronger interactions) with hTTR according to eq 1. Because of the directivity and great proportion of E_{ele} in E_{int}, it is the electrostatic interactions that make the ionized groups of the phenolic compounds have a dominant orientation in the T_4 binding channel of hTTR.

In addition to the electrostatic and cation−π interactions, some compounds also have hydrogen bonds with hTTR (Figure 4), and all of the compounds have hydrophobic interactions with hTTR (Figure S5, Supporting Information). However, the hydrophobic interactions do not have an impact on the orientitation of the chemicals in the hTTR entry port. If a compound has both electrostatic and cation−π interactions and hydrogen bonds with hTTR, the three kinds of interactions jointly determine the orientitation of the chemicals.

Development of the QSAR Model. The obtained optimum QSAR model is:

$$\log RP = -4.37 \times 10^{-1} - 1.26 \times 10^{-1} pK_a - 3.16 qO^-_{adj} + 1.84 \times 10^{-2} \log D \quad (7)$$

$$n_{training} = 38, \quad A = 2, \quad R^2_{training} = 0.86, \quad Q^2_{CUM} = 0.84, \quad RMSE_{training} = 0.51, \quad p < 1.0 \times 10^{-5}$$

where $n_{training}$ is the number of compounds in the training set, A is the number of PLS components, $R^2_{training}$ is the squared correlation coefficient between observed and fitted values, $RMSE_{training}$ is the root-mean-square error, and p is the significance level. These statistics indicate that the model has a high goodness-of-fit and robustness, according to the criteria ($Q^2 > 0.50$; $R^2 > 0.60$) of Golbraikh et al.[58] The predictive ability of the model was evaluated by the three external validation sets. The statistics for validation set I are $n_{EXT} = 9$, external explained variance $Q^2_{EXT} = 0.93$, $R^2_{EXT} = 0.95$, and $RMSE_{EXT} = 0.32$ (Figure S6, Supporting Information). As the experimental protocols of validation sets II and III are different from that of the training set, linear correlation coefficients between the predicted and observed log RP values are calculated, which are 0.98 ($p < 0.0001$) and 0.81 ($p < 0.0005$) for validation sets II (Figure S7, Supporting Information) and III (Figure S8, Supporting Information), respectively. These results indicate that the developed QSAR model has good predictive ability. The AD of the model indicates that all of the compounds in both the training set and the validation sets are in the domain (Figure S9, Supporting Information), implying that the training set has good representativeness. The QSAR models based on the pK_a values from Discovery Studio 2.5.5 and SciFinder (Table S5, Supporting Information) are similar to the current model.

According to the variable importance in the projection (VIP) values listed in Table S6 (Supporting Information), pK_a is the most important parameter in explaining log RP. It has a negative coefficient in the model, which encodes the information that the anionic forms of the compounds bind stronger than the neutral forms. As far as we know, this is the first report to include pK_a as a key descriptor in QSAR modeling of EDCs. qO^-_{adj} is the second important predictor variable for explaining logRP. According to the QSAR model, a more negative value of qO^-_{adj} leads to a higher log RP value, as a compound with a more negative value of qO^-_{adj} has stronger electrostatic interactions between the $-O^-/-OH$ group and hTTR. log D is also a descriptor for proteinophilic property,[38,59] and it may characterize hydrophobic interactions between the phenolic compounds and hTTR in the model.

It deserves mentioning that the pK_a values of the compounds in the binding site can be different from those in water solutions.[60,61] If the pK_a values in the binding site are used in the modeling, the resulting QSAR model can be different. Currently, it is a challenge to calculate the pK_a values in the binding site, which needs further studies.

Implications. Among the 140,000 commercially used chemicals that have been preregistered by the REACH regulation, 14,332 chemicals may ionize to form anions under normal physiological pH conditions (~7.4 for human plasma).[62] pK_a values for ionizable compounds with $-SO_3H$, $-SO_2H$, and $-COOH$ as end groups are usually <7.4,[63] and pK_a values for the $-OH$ group in phenolic compounds are usually <10.[64] If the pK_a of a chemical is <10.4, more than 1% of the chemical exists in the form of anions under pH 7.4. Thus, those chemicals with ionizable groups like $-OH$, $-SO_3H$, $-SO_2H$, and $-COOH$, and with the pK_a values of <10.4, deserve special attention when screening high-priority hTTR disruptors.

In this study, we found that the directional electrostatic interactions dominate the binding between the anionic forms of the phenolic compounds and the protonated alkaline residues in the hTTR ligand-binding domain. There are two prerequisites for the electrostatic interactions: ionization of ligands and protonation or deprotonation of alkaline or acidic residues in the ligand-binding domain of macromolecules under physiological pH conditions. If the two key prerequisites are triggered simultaneously for a given endocrine system, the influence of chemical ionization should not be neglected when screening potential endocrine disruptors. For example, arginine and lysine (alkaline residues) in the ligand-binding domain of human thyroxine-binding globulin (hTBG) are protonated under physiological pH conditions. If disruptors of hTBG can also ionize under the same pH condition, the binding interactions with hTBG should also depend on the chemical forms of the disruptors. Thus, the mechanism found in this study is of great importance for the development of *in silico*, *in chemical*, and *in vitro* assay and screening methods for potential endocrine disruptors.

■ ASSOCIATED CONTENT

Ⓢ Supporting Information

Interaction energy values; a list of noncovalent binding forces in the hTTR crystal structures; the surface distribution of electrostatic potential for representative molecules; comparison of E_{ele} and E_{vdw} in E_{int}; figures indicating hydrophobic interactions, the correlation between observed and predicted log RP values, and the applicability domain of the QSAR model; and values of variable importance in the projection and of the molecular descriptors involved in the QSAR model. This material is available free of charge via the Internet at http://pubs.acs.org.

■ AUTHOR INFORMATION

Corresponding Author

*Phone/Fax: +86-411-8470 6269. E-mail: jwchen@dlut.edu.cn.

Funding

The study was supported by National Basic Research Program of China (2013CB430403), National Natural Science Founda-

tion of China (21137001), and High-Tech Research and Development Program of China (2012AA06A301).

Notes

The authors declare no competing financial interest.

■ ACKNOWLEDGMENTS

We thank Professor Dr. Willie Peijnenburg for help in improving this manuscript.

■ ABBREVIATIONS

AD, applicability domain; DIO, deiodinases; EDCs, endocrine disrupting chemicals; E_{ele}, electrostatic interaction energy; E_{int}, interaction energy; E_{vdw}, van der Waals interaction energy; HO-PBDEs, hydroxylated polybrominated diphenyl ethers; hTTR, human transthyretin; IC_{50}, half-maximal inhibitory concentration; NIS, sodium/iodide symporter; QM/MM, quantum mechanics/molecular mechanics; QSAR, quantitative structure−activity relationship; REACH, Registration, Evaluation, and Authorization, and Restriction of Chemicals; RMSD, root mean square deviation; *RP*, relative competing potency; T_3, 3,3′,5-triiodo-L-thyronine; T_4, 3,3′,5,5′-tetraiodo-L-thyronine; TBG, thyroxine-binding globulin; TDCs, thyroid-disrupting chemicals; THs, thyroid hormones; TPO, thyroperoxidase; TR, thyroid receptor; TRH, thyrotropin-releasing hormone; TSH, thyroid-stimulating hormone; UGTs, glucuronosyltransferase; SULTs, sulfotransferase

■ REFERENCES

(1) Hulbert, A. J. (2000) Thyroid hormones and their effects: a new perspective. *Biol. Rev. Camb. Philos. Soc. 75*, 519−631.

(2) Patrick, L. (2009) Thyroid disruption: mechanism and clinical implications in human health. *Altern. Med. Rev. 14*, 326−346.

(3) Miller, M. D., Crofton, K. M., Rice, D. C., and Zoeller, R. T. (2009) Thyroid-disrupting chemicals: interpreting upstream biomarkers of adverse outcomes. *Environ. Health Perspect. 117*, 1033−1041.

(4) Boas, M., Feldt-Rasmussen, U., Skakkebaek, N. E., and Main, K. M. (2006) Environmental chemicals and thyroid function. *Eur. J. Endocrinol. 154*, 599−611.

(5) Organisation for Economic Co-operation and Development (2012) Detailed Review Paper on the State of the Science on Novel in Vitro and in Vivo Screening and Testing Methods and Endpoints for Evaluating Endocrine Disruptors, *Technical Report for OECD Environment*, Health and Safety Publications Series on Testing and Assessment No. 178, pp 88, OECD, Paris, France.

(6) Ren, X. M., and Guo, L. H. (2012) Assessment of the binding of hydroxylated polybrominated diphenyl ethers to thyroid hormone transport proteins using a site-specific fluorescence probe. *Environ. Sci. Technol. 46*, 4633−4640.

(7) Cheek, A. O., Kow, K., Chen, J., and McLachlan, J. A. (1999) Potential mechanisms of thyroid disruption in humans: interaction of organochlorine compounds with thyroid receptor, transthyretin, and thyroid-binding globulin. *Environ. Health Perspect. 107*, 273−278.

(8) Kovarich, S., Papa, E., and Gramatica, P. (2011) QSAR classification models for the prediction of endocrine disrupting activity of brominated flame retardants. *J. Hazard Mater. 190*, 106−112.

(9) Cronin, M. T. D., Zhao, Y. H., and Yu, R. L. (2000) pH-Dependence and QSAR analysis of the toxicity of phenols and anilines to *Daphnia magna*. *Environ. Toxicol. 15*, 140−148.

(10) Zhang, H. B. (2005) A QSAR study of the brain/blood partition coefficients on the basis of pK_a values. *QSAR Comb. Sci. 25*, 15−24.

(11) Zhao, Y. H., Yuan, X., Su, L. M., Qin, W. C., and Abraham, M. H. (2009) Classification of toxicity of phenols to *Tetrahymena pyriformis* and subsequent derivation of QSARs from hydrophobic, ionization and electronic parameters. *Chemosphere 75*, 866−871.

(12) Rendal, C., Kusk, K. O., and Trapp, S. (2011) Optimal choice of pH for toxicity and bioaccumulation studies of ionizing organic chemicals. *Environ. Toxicol. Chem. 30*, 2395−2406.

(13) Won, C. M. (1992) Kinetics of degradation of levothyroxine in aqueous solution and in solid state. *Pharm. Res. 9*, 131−137.

(14) Connelly, S., Choi, S., Johnson, S. M., Kelly, J. W., and Wilson, I. A. (2010) Structure-based design of kinetic stabilizers that ameliorate the transthyretin amyloidoses. *Curr. Opin. Struct. Biol. 20*, 54−62.

(15) Somack, R., Andrea, T. A., and Jorgensen, E. C. (1982) Thyroid hormone binding to human serum prealbumin and rat liver nuclear receptor: kinetics, contribution of the hormone phenolic hydroxyl group, and accommodation of hormone side-chain bulk. *Biochemistry 21*, 163−170.

(16) Berg, N., De Wever, B., Fuchs, H. W., Gaca, M., Krul, C., and Roggen, E. L. (2011) Toxicology in the 21st century–working our way towards a visionary reality. *Toxicol. in Vitro 25*, 874−881.

(17) Kavlock, R., and Dix, D. (2010) Computational toxicology as implemented by the U.S. EPA: providing high throughput decision support tools for screening and assessing chemical exposure, hazard and risk. *J. Toxicol. Environ. Health, Part B 13*, 197−217.

(18) Cronin, M. T. D., Bajot, F., Enoch, S. J., Madden, J. C., Roberts, D. W., and Schwöbel, J. (2009) The *in chemico-in silico* interface: challenges for integrating experimental and computational chemistry to identify toxicity. *Altern. Lab. Anim. 37*, 513−521.

(19) Castello, P., and Worth, A. (2011) *Information Sources and Databases on Endocrine Active Substances*, Technical Report for the Office for Official Publications of the European Union, pp 9−11, Office for Official Publications of the European Union, Luxembourg.

(20) Papa, E., Kovarich, S., and Gramatica, P. (2010) QSAR modeling and prediction of the endocrine-disrupting potencies of brominated flame retardants. *Chem. Res. Toxicol. 23*, 946−954.

(21) Yang, W. H., Shen, S., Mu, L. L., and Yu, H. X. (2011) Structure-activity relationship study on the binding of PBDEs with thyroxine transport proteins. *Environ. Toxicol. Chem. 30*, 2431−2439.

(22) Lans, M. C., Klasson-Wehler, E., Willemsen, M., Meussen, E., Safe, S., and Brouwer, A. (1993) Structure-dependent competitive interaction of hydroxy-polychlorobiphenyls, -dibenzo-p-dioxins and -dibenzofurans with human transthyretin. *Chem.-Biol. Interact. 88*, 7−21.

(23) Meerts, I. A., van Zanden, J. J., Luijks, E. A., van Leeuwen-Bol, I., Marsh, G., Jakobsson, E., Bergman, A., and Brouwer, A. (2000) Potent competitive interactions of some brominated flame retardants and related compounds with human transthyretin in vitro. *Toxicol. Sci. 56*, 95−104.

(24) Legler, J., Cenijn, P. H., Malmberg, T., Bergman, Å., and Brouwer, A. (2002) Determination of the endocrine disrupting potency of hydroxylated PCBs and flame retardants with in vitro bioassays. *Organohalog. Compd. 56*, 53−56.

(25) Hamers, T., Kamstra, J. H., Sonneveld, E., Murk, A. J., Kester, M. H., Andersson, P. L, Legler, J., and Brouwer, A. (2006) In vitro profiling of the endocrine-disrupting potency of brominated flame retardants. *Toxicol. Sci. 92*, 157−173.

(26) Harju, M., Hamers, T., Kamstra, J. H., Sonneveld, E., Boon, J. P., Tysklind, M., and Andersson, P. L. (2007) Quantitative structure-activity relationship modeling on in vitro endocrine effects and metabolic stability involving 26 selected brominated flame retardants. *Environ. Toxicol. Chem. 26*, 816−826.

(27) Hamers, T., Kamstra, J. H., Sonneveld, E., Murk, A. J., Visser, T. J., Van Velzen, M. J., Brouwer, A., and Bergman, A. (2008) Biotransformation of brominated flame retardants into potentially endocrine-disrupting metabolites, with special attention to 2,2′,4,4′-tetrabromodiphenyl ether (BDE-47). *Mol. Nutr. Food Res. 52*, 284−298.

(28) Van Den Berg, K. J. (1990) Interaction of chlorinated phenols with thyroxine binding sites of human transthyretin, albumin and thyroid binding globulin. *Chem.-Biol. Interact. 76*, 63−75.

(29) Cao, J., Lin, Y., Guo, L. H., Zhang, A. Q., Wei, Y., and Yang, Y. (2010) Structure-based investigation on the binding interaction of

hydroxylated polybrominated diphenyl ethers with thyroxine transport proteins. *Toxicology 277*, 20−28.
(30) Liu, H. X., Papa, E., and Gramatica, P. (2008) Evaluation and QSAR modeling on multiple endpoints of estrogen activity based on different bioassays. *Chemosphere 70*, 1889−1897.
(31) Wallace, A. C., Laskowski, R. A., and Thornton, J. M. (1995) LIGPLOT: a program to generate schematic of protein-ligand interactions. *Protein Eng. 8*, 127−134.
(32) Burykin, A., Schutz, C. N., Villá, J., and Warshel, A. (2002) Simulations of ion current in realistic models of ion channels: the KcsA potassium channel. *Proteins 47*, 265−280.
(33) RCSB Protein Data Bank Home Page, http://www.rcsb.org/pdb/home/home.do (accessed Mar 27, 2012).
(34) Sgrignani, J., Bonaccini, C., Grazioso, G., Chioccioli, M., Cavalli, A., and Gratteri, P. (2009) Insights into docking and scoring neuronal alpha4beta2 nicotinic receptor agonists using molecular dynamics simulations and QM/MM calculations. *J. Comput. Chem. 30*, 2443−2454.
(35) Yu, Y., Li, W. G., Chen, Z., Cao, H., Yang, H., Jiang, H., and Xu, T. L. (2011) Atomic level characterization of the nonproton ligand-sensing domain of ASIC3 channels. *J. Biol. Chem. 286*, 24996−25006.
(36) Baber, J. C., Thompson, D. C., Cross, J. B., and Humblet, C. (2009) GARD: a generally applicable replacement for RMSD. *J. Chem. Inf. Model. 49*, 1889−1900.
(37) Sotriffer, C. A., Gohlke, H., and Klebe, G. (2002) Docking into knowledge-based potential fields: a comparative evaluation of DrugScore. *J. Med. Chem. 45*, 1967−1970.
(38) Todeschini, R., and Consonni, V. (2009) *Molecular Descriptors for Chemoinformatics*, 2nd ed., pp 590−601, Wiley-VCH, Weinheim, Germany.
(39) (2013) *SPARC*, v4.6, ARChem, Danielsville, GA, http://ibmlc2.chem.uga.edu/sparc (accessed Mar 19, 2013).
(40) Dearden, J., and Worth, A. (2007) *In Silico Prediction of Physicochemical Properties*, EUR-Scientific and Technical Research Reports, pp 25−26, Office for Official Publications of the European Communities, Luxembourg.
(41) Liao, C., and Nicklaus, M. C. (2009) Comparison of nine programs predicting pK(a) values of pharmaceutical substances. *J. Chem. Inf. Model. 49*, 2801−2812.
(42) Arp, H. P., Droge, S. T., Endo, S., Giger, W., Goss, K. U., Hawthorne, S. B., Mabury, S. A., Mayer, P., McLachlan, M. S., Pankow, J. F., Schwarzenbach, R. P., Wania, F., and Xing, B. S. (2010) More of EPA's SPARC online calculator–the need for high-quality predictions of chemical properties. *Environ. Sci. Technol. 44*, 4400−4401.
(43) (2012) *Estimation Programs Interface Suite for Microsoft® Windows*, v 4.10, United States Environmental Protection Agency, Washington, DC.
(44) (2012) *DRAGON (Software for Molecular Descriptor Calculation)*, version 6.0; Talete srl, Milano, Italy.
(45) Frisch, M. J., Trucks, G. W., Schlegel, H. B., Scuseria, G. E., Robb, M. A., Cheeseman, J. R., Scalmani, G., Barone, V., Mennucci, B., Petersson, G. A., Nakatsuji, H., Caricato, M., Li, X., Hratchian, H. P., Izmaylov, A. F., Bloino, J., Zheng, G., Sonnenberg, J. L., Hada, M., Ehara, M., Toyota, K., Fukuda, R., Hasegawa, J., Ishida, M., Nakajima, T., Honda, Y., Kitao, O., Nakai, H., Vreven, T., Montgomery, J. A., Peralta, J. E., Jr., Ogliaro, F., Bearpark, M., Heyd, J. J., Brothers, E., Kudin, K. N., Staroverov, V. N., Kobayashi, R., Normand, J., Raghavachari, K., Rendell, A., Burant, J. C., Iyengar, S. S., Tomasi, J., Cossi, M., Rega, N., Millam, J. M., Klene, M., Knox, J. E., Cross, J. B., Bakken, V., Adamo, C., Jaramillo, J., Gomperts, R., Stratmann, R. E., Yazyev, O., Austin, A. J., Cammi, R., Pomelli, C., Ochterski, J. W., Martin, R. L., Morokuma, K., Zakrzewski, V. G., Voth, G. A., Salvador, P., Dannenberg, J. J., Dapprich, S., Daniels, A. D., Farkas, O., Foresman, J. B., Ortiz, J. V., Cioslowski, J., and Fox, D. J. (2009) *Gaussian 09*, revision a.02, Gaussian, Inc., Wallingford, CT.
(46) Li, F., Li, X. H., Shao, J. P., Chi, P., Chen, J. W., and Wang, Z. J. (2010) Estrogenic activity of anthraquinone derivatives: in vitro and in silico studies. *Chem. Res. Toxicol. 23*, 1349−1355.
(47) Chen, J. W., Quan, X., Peijnenburg, W. J. G. M., and Yang, F. L. (2001) Quantitative structure-property relationships (QSPRs) on direct photolysis quantum yields of PCDDs. *Chemosphere 43*, 235−241.
(48) Schüürmann, G., Ebert, R. U., Chen, J. W., Wang, B., and Kühne, R. (2008) External validation and prediction employing the predictive squared correlation coefficient - test set activity mean vs training set activity mean. *J. Chem. Inf. Model 48*, 2140−2145.
(49) Pullakhandam, R., Srinivas, P. N., Nair, M. K., and Reddy, G. B. (2009) Binding and stabilization of transthyretin by curcumin. *Arch. Biemoch. Biophys. 485*, 115−119.
(50) Kumar, S., and Nussinov, R. (2002) Relationship between ion pair geometries and electrostatic strengths in proteins. *Biophys. J. 83*, 1595−1612.
(51) Muegge, I., Tao, H., and Warshel, A. (1997) A fast estimate of electrostatic group contributions to the free energy of protein-inhibitor binding. *Protein Eng. 10*, 1363−1372.
(52) Schutz, C. N., and Warshel, A. (2001) What are the dielectric "constants" of proteins and how to validate electrostatic models? *Proteins 44*, 400−417.
(53) Warshel, A., Sharma, P. K., Kato, M., Xiang, Y., Liu, H., and Olsson, M. H. (2006) Electrostatic basis for enzyme catalysis. *Chem. Rev. 106*, 3210−3235.
(54) Banerjee, A., Hussainzada, N., Khandelwal, A., and Swaan, P. W. (2008) Electrostatic and potential cation-p forces may guide the interaction of extracellular loop III with Na+ and bile acids for human apical Na+-dependent bile acid transporter. *Biochem. J. 410*, 391−400.
(55) Zacharias, N., and Dougherty, D. A. (2002) Cation-pi interactions in ligand recognition and catalysis. *Trends Pharmacol. Sci. 23*, 281−287.
(56) Mecozzi, S., West, A. P., Jr., and Dougherty, D. A. (1996) Cation-pi interactions in aromatics of biological and medicinal interest: electrostatic potential surfaces as a useful qualitative guide. *Proc. Natl. Acad. Sci. U.S.A. 93*, 10566−10571.
(57) Wheeler, S. E., and Houk, K. N. (2009) Substituent effects in cation/pi interactions and electrostatic potentials above the centers of substituted benzenes are due primarily to through-space effects of the substituents. *J. Am. Chem. Soc. 131*, 3126−3127.
(58) Golbraikh, A., Shen, M., Xiao, Z., Xiao, Y. D., Lee, K. H., and Tropsha, A. (2003) Rational selection of training and test sets for the development of validated QSAR models. *J. Comput.-Aided. Mol. Des. 17*, 241−253.
(59) Bhal, S. K., Kassam, K., Peirson, I. G., and Pearl, G. M. (2007) The rule of five revisited: applying log D in place of log P in drug-likeness filters. *Mol. Pharmaceutics 4*, 556−560.
(60) Borštnar, R., Repič, M., Kamerlin, S. C. L., Vianello, R., and Mavri, J. (2012) Computational study of the pKa values of potential catalytic residues in the active site of monoamine oxidase B. *J. Chem. Theory Comput. 8*, 3864−3870.
(61) Il'ichev, Y. V., Perry, J. L., and Simon, J. D. (2002) Interaction of ochratoxin A with human serum albumin preferential binding of the dianion and pH effects. *J. Phys. Chem. B 106*, 452−459.
(62) Daginnus, K. (2010) *Characterisation of the REACH Pre-Registered Substances List by Chemical Structure and Physicochemical Properties*, EUR-Scientific and Technical Research Reports, pp 16, Office for Official Publications of the European Communities, Luxembourg.
(63) Franco, A., Ferranti, A., Davidsen, C., and Trapp, S. (2010) An unexpected challenge: ionizable compounds in the REACH chemical space. *Int. J. Life Cycle Assess. 15*, 321−332.
(64) Fox, M. A., and Whitesell, J. K. (2004) Understanding Organic Reactions, in *Organic Chemistry*, 3th ed., pp 294−295, Jones & Bartlett Publishers, Burlington, MA.